Int. J. Electrochem. Sci., 13 **(2018)** 9931 – 9941, doi: 10.20964/2018.10.32

International Journal of ELECTROCHEMICAL SCIENCE
www.electrochemsci.org

Fabrication of Copper Oxide Thin Films by Galvanostatic Deposition from Weakly Acidic Solutions

Mansoureh Keikhaei[*], *Masaya Ichimura*

Department of Electrical and Mechanical Engineering, Nagoya Institute of Technology, Gokiso, Showa, Nagoya 466-8555, Japan
[*]E-mail: keykhaei@gmail.com

Received: 30 May 2018 / *Accepted:* 11 July 2018 / *Published:* 1 September 2018

Copper oxide thin films are deposited low pH (<6) and low and high temperatures (10°C and 60°C), using cathodic electrochemical deposition. The effects of the deposition current densities are studied in a range including values high enough to electrolyze water, promoting hydrogen bubbles generation. The influences of deposition variables on film composition and structural, morphological, and optical properties are investigated. Auger electron spectroscopy results indicate the fabrication of both Cu_2O and CuO, which is consistent with the results of Raman spectroscopy. X-ray diffraction patterns show (111) and (220) peaks related to Cu_2O for the samples deposited at 60°C, whereas samples deposited at low temperatures are almost amorphous.

Keywords: electrochemical deposition, copper oxide, thin films, water electrolysis and band gap

1. INTRODUCTION

Modern technology requires the deposition of thin films, which is the basis of development in solid state electronics. In this way, the growth of semiconductor thin films is one of the key technologies for pn-junction-based devices such as diodes, transistors, solar cells and light emitting devices [1–3]. Copper oxide is an attractive material for solar energy applications. Both cupric oxide (CuO) and cuprous oxide (Cu_2O) are intrinsically p-type semiconductors with band gaps of 1.3–2.1 eV for CuO and 2.1–2.6 eV for Cu_2O [4].

In the past decades, numerous approaches have been developed for the fabrication of copper oxide such as chemical vapor deposition, sputtering [5], and sol–gel process [6]. Electrochemical deposition (ECD) has been attracting much attention as a method for the preparation of semiconducting thin layers on conducting substrates owing to its good controllability of growth rate through the control of various deposition parameters, economy, and environmental-friendly processing [7–8]. ECD of copper oxide has been performed through both anodic [6, 9–11] and cathodic

depositions [2,8,12,13]. In the cathodic deposition, thin films are deposited mostly at high temperature (typically around 60°C), high pH (>10), and for several tens of min [7,12]. In contrast, there are few reports of ECD performed at high temperature and low pH (< 5) [8,14,15]. According to previous studies, Cu was also deposited on a Pt substrate under high cathodic deposition currents (−5 mA/cm^2), while at a low negative deposition currents, (111)-oriented Cu_2O was deposited [14]. To the best of our knowledge, there are no reports on the deposition of Cu_2O or CuO thin films at low temperature, low pH, and high cathodic current (e.g., >−5 mA/cm^2). The copper oxide deposition mechanism by reduction in aqueous copper nitrate solution is generally known to proceed through the following steps [8]:

$$Cu(NO_3)_2 \rightarrow Cu^{2+} + 2NO_3 \quad (1)$$

$$NO_3^- + 2H_2O + 2e\text{-} \rightarrow NO_2^- + 2OH \quad (2)$$

$$O_2 + 2H_2O + 4e^- \rightarrow 4OH \quad (3)$$

$$Cu^{2+} + 2OH^- \rightarrow Cu(OH)_2 \quad (4)$$

$$Cu(OH)_2 \rightarrow CuO + H_2O \quad (5)$$

$$2Cu + 2e^- + 2OH^- \rightarrow Cu_2O + H_2O \quad (6)$$

Reactions (2) and (3) produce OH^- ions, which locally enhance the pH at the interface. Then, the OH^- ions react with metal ion Cu^+ in the solution. Reactions (4) and (5) show the CuO deposition mechanism, whereas reaction (6) displays the Cu_2O deposition reaction. In typical conditions, Cu_2O is formed with OH^- in the solution with high pH (>10), and the spontaneous formation of $Cu(OH)_2$ is suppressed by the addition of a complexing agent (lactic acid). Concomitantly to reactions (2) and (3), the generation of OH^- ions from the electrolysis of water may also occur as follows [16]:

$$2H_2O + 2e^- \rightarrow H_2 + 2OH^- \quad (7)$$

However, to the best of our knowledge, there is no report on fabricating copper oxide thin films using such mechanism. It has been generally assumed that the film surface will be roughened by the bubbles generated during water electrolysis, and thus the potential resulting in the promotion of Reaction (7) is usually avoided. However, it was recently reported that NiO thin films with smooth surface morphology can be deposited by ECD involving water electrolysis [17].

In the present investigation, copper oxide thin films are deposited by galvanostatic ECD on indium tin oxide (ITO)-coated glass substrates at low pH (<6) and at both low and high temperatures (10°C and 60°C). In heterostructure fabrication by ECD, the material on the first layer sometimes reacts with the deposition solution of the second layer, eventually resulting in a disordered interface. Such reactions may be prevented by adjustment of the solution pH, thereby making deposition in a

different pH range convenient. The deposition time was adjusted to be short, and the effects of the deposition current densities were investigated in a range that included values high enough to electrolyze water and generate hydrogen bubbles. As shown in the next sections, we succeeded in depositing copper oxide thin films based on Reactions (1)–(7). Moreover, we found that copper oxide films deposited at 10°C were almost amorphous but still exhibited clear optical absorption edge and p-type photoresponse.

2. EXPERIMENTAL

2.1. Preparation of copper oxide films

Copper oxide thin films were grown by the ECD technique using a three-electrode cell and a Hokutodenko HA151-B potentiostat/galvanostat. ITO-coated glass substrate (approximately 10 Ω/ square) was used as the working electrode, an Ag/AgCl electrode as the reference electrode and a platinum sheet as the counter electrode. ITO-coated glass substrates were cleaned in acetone and rinsed thoroughly with purified water. The deposited area was 1 cm × 1 cm. The deposition of copper oxide thin films was performed in the presence of an aqueous electrolyte containing equimolar concentrations (0.4 M) of $Cu(NO_3)_2 \cdot 6H_2O$ and and L(+)lactic acid, at cathodic current densities of −2, −5, −7, −8, and −10 mA/cm^2. The deposition time was 20 s. The solution pH was adjusted to 2.45, 4.0, and 5.8 by addition of NaOH solution. The deposition bath temperature was set at two different temperatures, 10°C and 60 °C.

2.2 Characterization of the deposited films

Cyclic voltammetry (CV) was conducted at a scan rate of 20 mV/s, between −2 and 0.5 V *vs.* Ag/AgCl, controlled by a Hokutodenko HA151-B potentiostat/galvanostat. Layer thickness values were determined by an Accretech Surfcom-1400D profilometer. The compositional analysis of the deposited films was performed with Auger electron spectroscopy (AES), using a JEOL JAMP 9500F Auger microprobe, at probe current of 20 mA and 10 kV of voltage operation. Argon-ion etching with current of 20 mA and acceleration voltage of 3 kV was employed to sputter. O/Cu ratios were calculated using a commercially available standard CuO chemical as reference. Initially, the peak-to-peak intensity ratio (Cu/O) was obtained from the AES spectrum of the sample. Then, the ratio was divided by the Cu/O ratio of the AES data of the reference. Scanning electron microscopy (SEM) images at 5000× magnification were also taken using JAMP 9500F microprobe. X-ray diffraction (XRD) experiments were performed with a SmartLab X-ray diffractometer (Rigaku) using a CuKα radiation source. Raman spectra were recorded under the excitation laser wavelength of 532 nm and laser power of 6.1 mW by using a Jasco NRS-3300 Raman spectroscope. The optical transmittance measurement was performed using a Jasco U-570 UV/VIS/NIR spectrometer using ITO substrate transmittance as reference. The photoelectrochemical (PEC) experiment was performed voltammetrically in a three-electrode cell with the fabricated thin films as working electrode and a 0.1 M Na_2SO_4 aqueous solution as electrolyte. Optical excitation of the films was done by radiating light

(100 mW/cm^2) intermittently at 5 s intervals, using an Abet technologies 10500 solar simulator, while the film was polarized within a range of −1.0 to 1.0 V at a scan rate of 5 mV/s.

3. RESULTS AND DISCUSSION

3.1 Electrochemistry

CV was used to characterize the electrochemical behavior of our solution [0.4 M $Cu(NO_3)_2$, L(+)lactic acid and NaOH] in a pH value adjusted to 5.8. Figure 1 shows typical voltammetric curves for two temperatures, 10°C and 60°C. At 10°C (curve (a)), a reduction peak is evident at about −0.7 V with a reduction current density of nearly −0.6 mA/cm^2. At 60°C, there are significant shifts of the reduction peaks that are observed at about −0.5, −0.7, and −0.9 V, with current densities from −1.2 to −1 mA/cm^2. We associate all those reduction peaks to Reactions (2) or (3), which are dominant in the deposition at relatively low cathodic potentials (i.e., low current densities).

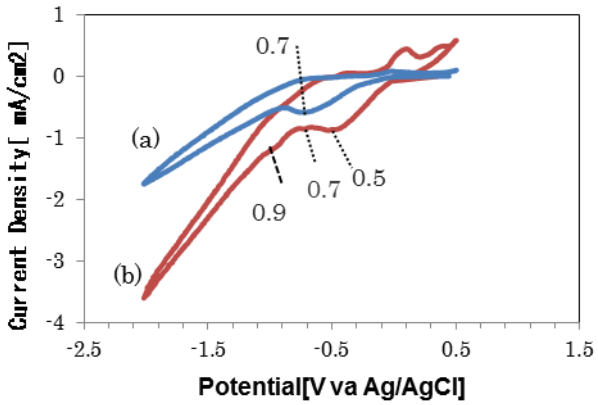

Figure 1. CV curves of the deposition solution containing 0.4 M $Cu(NO_3)_2$, L(+)Lactic acid and NaOH, at pH 5.8, and at (a) 10°C and (b) 60°C.

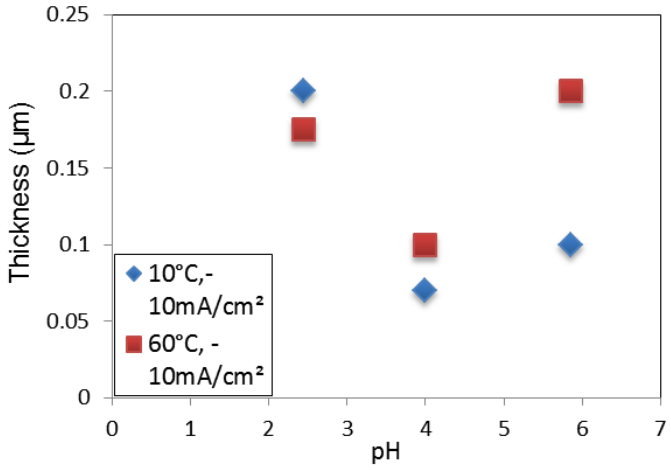

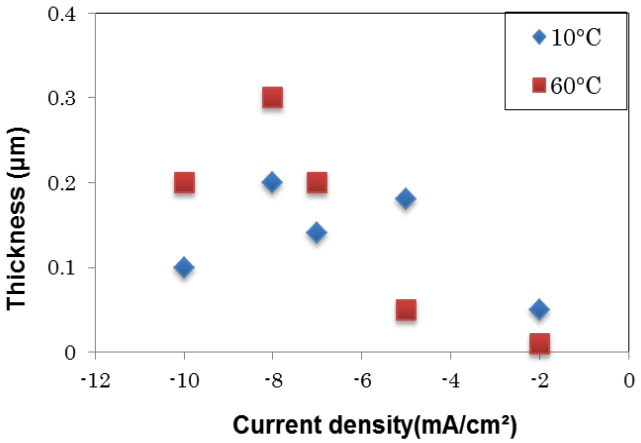

Figure 2. (a) Film thicknesses of copper oxide films versus pH, deposited with a current density of −10 mA/cm² and deposition time of 20s. (b) Film thicknesses obtained at different current densities, pH pf 5.8, and deposition time of 20s.

At more cathodic potentials (i.e., higher negative current densities), electrolysis of water [Reaction (7)] will be dominant instead of Reaction (2). The latter reaction is especially active at current densities over −5.0 mA/cm^2, at which hydrogen bubbles are generated. At low temperature, less hydrogen bubbles were observed than at high temperature.

The variation of film thickness with pH (from 2.5 to 5.8) at constant current density of −10 mA/cm² is shown in Fig. 2(a), as well as the dependence of the thickness on current density at pH 5.8 in Fig. 2(b), at the two different bath temperatures tested. Fig 2(a) shows that there is no clear trend in the film thickness variation with pH at both temperatures. At low pH, the thickness was too nonuniform to evaluate it precisely. However, we obtained significantly more uniform films at pH 5.8, thicker at 60 °C than at 10 °C. The color of the films also changed with pH from dark yellow at 2.5 to light yellow at 5.8. From the dependence of the thickness shown in Fig2 (b), it is obvious that at low current density (−2 mA/cm²) there is no significant measurable film thickness at both temperatures tested. With the employment of larger deposition currents, the film color became a little reddish and then turned to dark yellow. The film surface was rather smooth when obtained using high current densities (from −7 to −10 mA/cm²).

3.2. Structure characterization

Exemplarily, AES results for the two samples, deposited at 10°C(−5 mA/cm^2), and 60°C (−10 mA/cm^2), are shown in Fig. 3. In these conditions, the signals of Cu and O are detected along with a small intensity peak attributed to indium signal. In some samples, significant signals of indium and carbon were observed and such samples were not subjected to any further characterization (carbon could be contained in the film because of lactic acid).

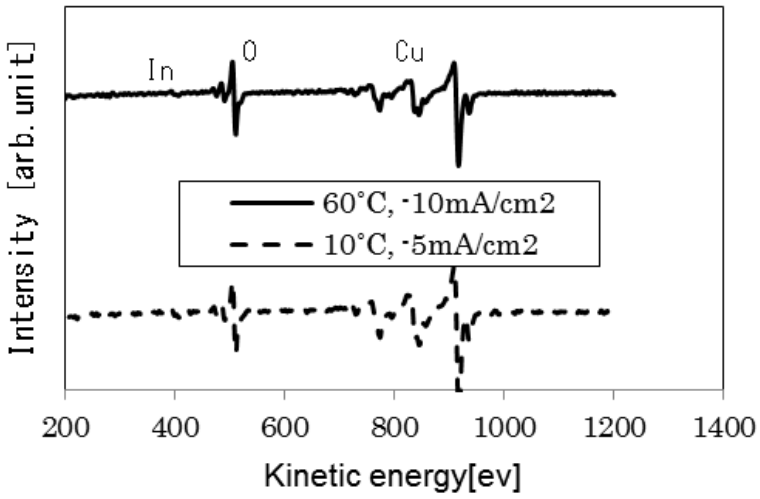

Figure 3. AES spectra for copper oxide films deposited at 60°C with current density of −10mA/cm^2, and for the film deposited at 10°C with current density −5mA/cm^2. The pH was adjusted to 5.8 in both cases.

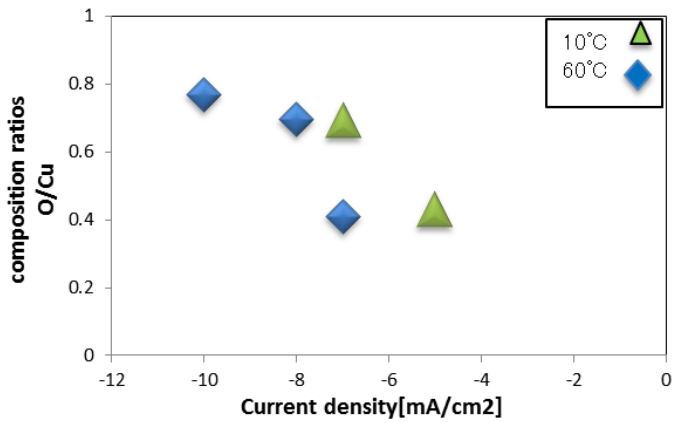

Figure 4. O/Cu Composition ratio for samples obtained at different current densities at 10°C and 60°C and pH 5.8.

Fig. 4 shows that O/Cu ratios for all the films are between 0.4 to 0.8. Therefore, the deposit will be a mixture of Cu_2O and CuO. With deposition current increment, the O/Cu ratio tends to increase, indicating more CuO in the film composition.

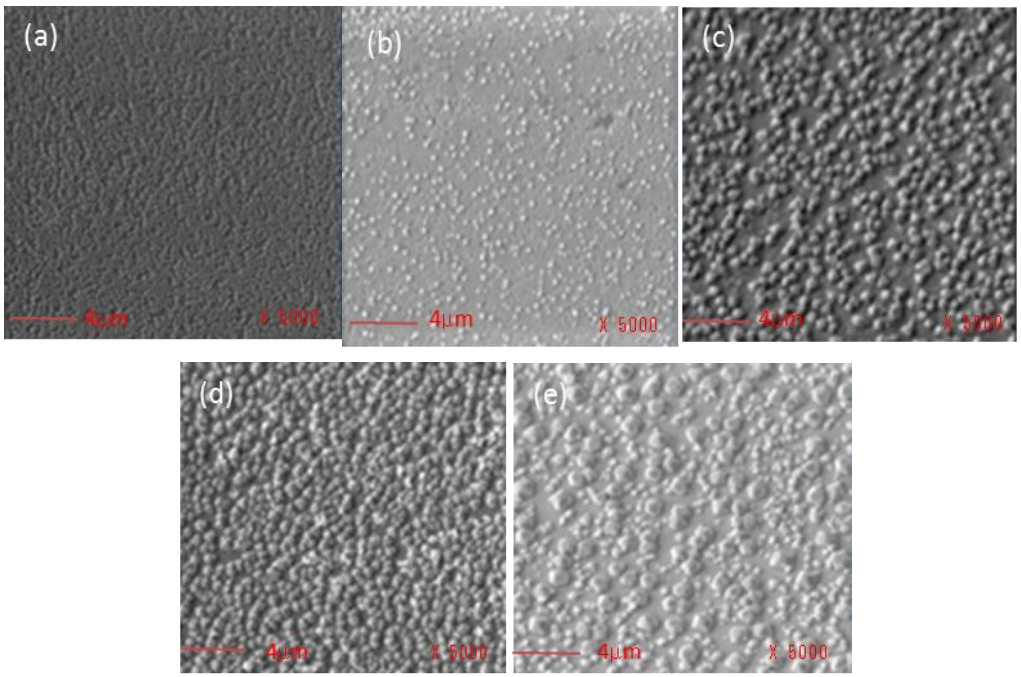

Figure 5. SEM images of the copper oxide films deposited at pH 5.8. The deposition temperatures and current densities are as follows: (a) 10°C, −5 mA/cm^2; (b) 10°C, −7 mA/cm^2; (c) 60°C, −7 mA/cm^2; (d) 60°C, −8 mA/cm^2; and (e) 60°C, −10 mA/cm^2.

SEM images for the films deposited at 10°C and 60 °C are shown in Fig. 5. For the samples deposited at 10°C, small grains (of around 200 nm) were observed on a continuous film. With the increase in temperature (at 60°C), the grains became bigger, (around 700−1000 nm in diameter) and tend to exhibit crystalline facets [2]. There is no significant variation of morphology by changing current at both temperatures tested. We found no clear influences on surface morphology eventually promoted by the hydrogen bubbles generation during the deposition upon large current density.

.

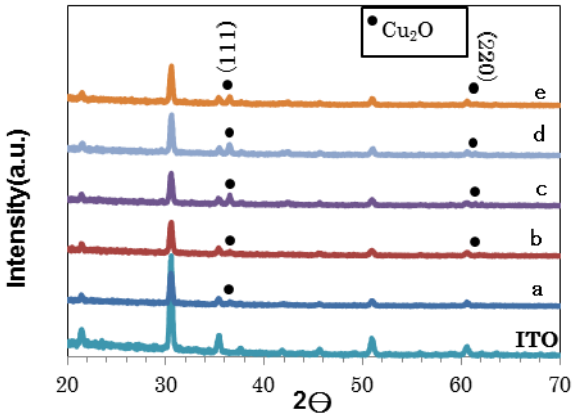

Figure 6. XRD patterns of copper oxide films deposited at pH 5.8. The deposition temperatures and current densities are as follows: (a) 10°C, −5 mA/cm^2; (b) 10°C, −7 mA/cm^2; (c) 60°C, −7 mA/cm^2; (d) 60°C, −8 mA/cm^2; and (e) 60°C, −10 mA/cm^2.

To clarify the structural properties, XRD has been performed and the results are shown in Fig. 6 for the films deposited at (a) 10°C, −5 mA/cm^2; (b) 10°C, −7 mA/cm^2; (c) 60°C, −7 mA/cm^2; (d) 60°C, −8 mA/cm^2; and (e) 60°C, -10 mA/cm^2. We observed peaks corresponding to Cu_2O (111) (2θ = 36.4°) and (220) (2θ = 61.0°) [3,18,19]. Practically, for the samples deposited at 10°C, the (111) diffraction peaks are of very low intensity and the (220) peak is not observable. In contrast, the (111) and (220) peaks are clearly observed for the samples deposited at 60°C. Thus, the formation of polycrystalline Cu_2O at 60°C was confirmed, but the films are almost amorphous when deposited at 10°C.

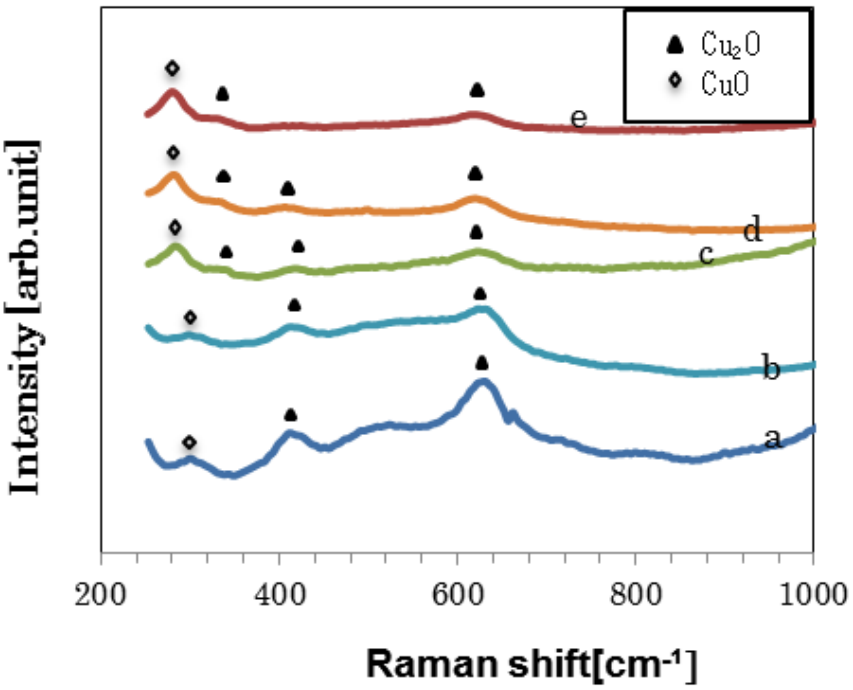

Figure 7. Raman spectra for copper oxide films deposited at pH 5.8. The deposition temperatures and current densities are as follows: (a) 10°C, −5 mA/cm^2; (b) 10°C, −7mA/cm^2; (c) 60°C, −7 mA/cm^2; (d) 60°C, −8 mA/cm^2; and (e) 60°C, −10 mA/cm^2.

To confirm the phase purity, Raman spectra were taken. Figure 7 reveals the Raman spectroscopy results for the samples obtained in the same conditions as shown in Fig. 6. For the samples deposited at 10°C (Samples (a) and (b)), the peak due to Cu_2O appears around 410 and 630 cm^{-1} [20–21], along with a weaker peak near 290 cm^{-1}, due to CuO. Thus, although XRD peaks are almost absent in those samples, one can conclude from the Raman data that the deposit is predominantly formed by Cu_2O. For the samples deposited at 60°C (Samples (c), (d), and (e)), weak Cu_2O peaks are observed, but another peak is observed near 279 cm^{-1}. This peak has been also attributed to CuO in a previous work [19].

3.3. Optoelectronic characterization

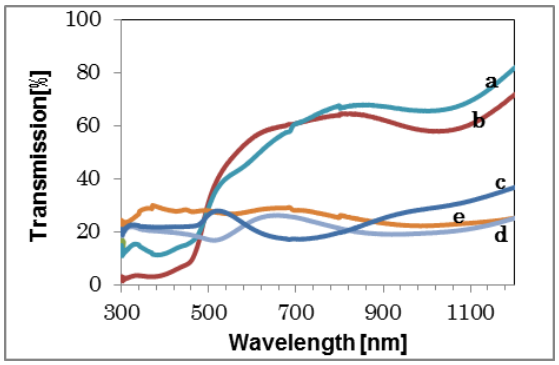

Figure 8. Optical transmission spectra for copper oxide films deposited at pH 5.8. The deposition temperatures and current densities are as follows: (a) 10°C, −5 mA/cm^2; (b) 10°C, −7 mA/cm^2; (c) 60°C, −7 mA/cm^2; (d) 60°C, −8 mA/cm^2; and (e) 60°C, −10 mA/cm^2.

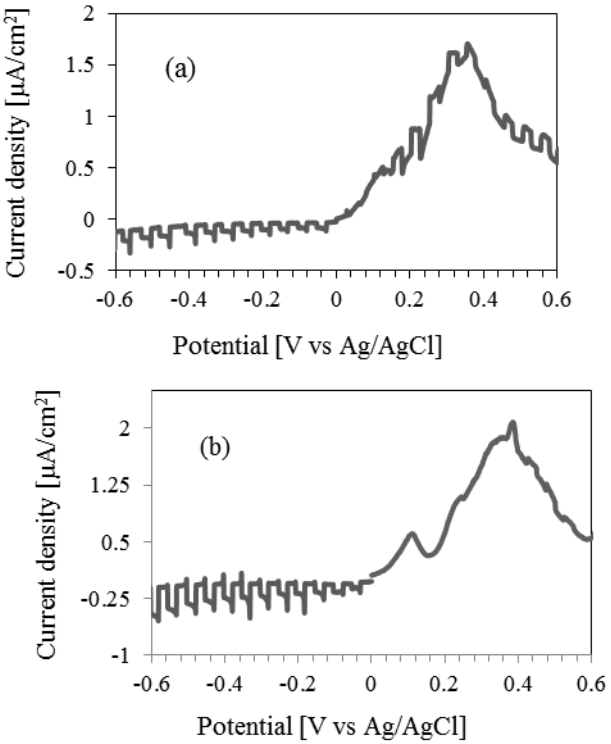

Figure 9. PEC measurements for copper oxide films deposited at pH 5.8. The deposition temperatures and current densities are as follows: (a) 60°C, −10 mA/cm^2 and (b) 10°C, −5 mA/cm^2.

Fig. 8 shows the optical transmission spectra for the films. The transmittance tends to decrease with increasing deposition temperature, and there is no clear absorption edge for the samples deposited at 60°C. This may occur because of the light scattering at rough surfaces. For samples deposited at 10°C (Samples (a) and (b)), the absorption edge appears near 530 nm. The bandgap calculated from the plot of $(\alpha h\nu)^2$ *vs.* $h\nu$, where α is the absorption coefficient and $h\nu$ the photon energy, is 2.2 eV for both Samples (a) and (b).

Fig. 9 depicts the PEC curves, showing the current density *vs.* potential responses for the samples deposited at (a) 60°C, −10 mA/cm^2 and (b) 10°C, −5 mA/cm^2. In Fig. 9 (b), a clear photoresponse was observed in the negative branch, which indicated that the electron is the minority carrier, i.e., the conduction type is p-type. In Fig. 9(a), a positive photoresponse was also observed, but the overall rectification properties were typical of p-type semiconductors. All the other samples characterized (not shown here) exhibited photocurrent responses similar to that of Fig. 9 (b).

The films deposited at 10°C with currents of −5 and −7 mA/cm^2 are almost amorphous according to the XRD results; however, those films exhibited a clear absorption edge and p-type photoresponse, suggesting that amorphous copper oxide deposited by ECD can also be a useful material for optoelectronic applications, such as solar cells.

4. CONCLUSION

In summary, p-type Cu_2O thin films were fabricated onto ITO-coated conducting glass substrates using galvanostatic ECD in a weakly acidic solution (<6) under large deposition current densities (≥−5 mA/cm^2). Under such conditions, OH^- ions were considered to be sourced from the water electrolysis. AES measurement results indicated deposition of both Cu_2O and CuO, which is consistent with the results of Raman spectroscopy. XRD studies revealed two peaks of Cu_2O, (111) and (220) for the samples deposited at 60°C, whereas the samples deposited at 10°C seemed almost amorphous. The optical transmittance decreased with increasing deposition temperature, and for the samples deposited at 10°C and −5 and −7 mA/cm^2, the band gap was estimated to be 2.2 eV.

ACKNOWLEDGEMENT
We would like to thank Ms. Miki Koyama for her technical assistance.

References

1. M.C. RAO, *Int. J. Modern. Phys*., 22 (2013) 576.
2. V. Dhanasekaran, T.Mahalingam, R. Chandramohan, J.K. Rhee and J.P. Chu, *Thin. Solid. Films*, 520 (2012) 6608.
3. V. Georgievaa and M. Ristovb, *Sol. Energy Mater. Sol. Cell*., 73 (2002) 67.
4. U. Rajalakshmi and R.Oommen, *Adv. Mater. Res*., 678 (2013) 118.
5. J. Mathur and M. Gupta, *IOSR J. Engineering,* 5 (2013) 55.
6. M.J. Siegfried and K.S. Choi, *J. Electrochem. Soc*., 154 (2007) 674.
7. K. Fujimoto, T. Oku, T. Akiyama and A. Suzuki, *J. Phys.: Conf. Series*, 433 (2013) 1.
8. J. Lee and Y. Tak, *Electrochem. Solid-State Lett.*, 3 (2000) 69.
9. C.H. Pyun and S.M. park, *J. Electrochem. Soc*., 133 (1986) 2024.
10. J.G. Becerra, R.C. Salvarezza and A.J. Arivia, *Electochim. Acta*, 33 (1988) 613.
11. V. Ashworth and D. Fairurst, *J. Electrochem. Soc*., 124 (1977) 506.
12. T.D. Golden, M.G. Shumsky, Y. Zhou, R.A. Vander Werf, R.A. Van Leeuwen and J.A. Switzer, *Chem. Mater*., 8 (1996) 2499.
13. D. Lu and K. Tanaka, *J. Electrochem. Soc*., 143 (1996) 2105.
14. J. Lee and Y. Tak, *Electrochem. Solid-State Lett.*, 2 (1999) 556.

15. H.H. Strehblow and B. Titze, *Electrochim. Acta*, 25 (1980) 839.
16. G.H.A. Theresa and P.V. Kamath, *Chem. Mater.,* 2 (2000) 2000.
17. M. Koyama and M. Ichimura, *Semicond. Sci. Technol*., 33 (2018) 055011.
18. J.Y. Zheng, A.P. Jadhav, G. Song, C.W. Kim and Y.S. Kang, *Thin. Solid. Films*, 524 (2012) 50.
19. A. Bello, D. Dodoo-Arshin, K. Makgopa, M. Fabiane and N. Manyala, *American J. Mater. Sci.*, 2 (2014) 63.
20. P. Poizot, C.J. Hung, M.P. Nikiforov, E.W. Bohannan and J. A. Switzer, *Electrochem. Solid-State Lett.*, 6 (2003) C21.
21. Y.G. Lee, J.R. Wang, M.J. Chuang , D.W. Chen and K.H. Hou, *Int. J. Electrochem. Sci.,* 12 (2017) 507.